

# EFFECTS OF MICROTEARING MODES ON THE EVOLUTION OF ELECTRON TEMPERATURE PROFILES IN HIGH COLLISIONALITY NSTX DISCHARGES

T. RAFIQ<sup>1</sup>, S. KAYE<sup>2</sup>, W. GUTTENFELDER<sup>2</sup>, J. WEILAND<sup>3</sup> and J. ANDERSON<sup>3</sup>

<sup>1</sup>Lehigh University, Bethlehem, PA, USA

<sup>2</sup>Princeton Plasma Physics Laboratory, Princeton, NJ, USA

<sup>3</sup>Chalmers University of Technology and EURATOM-VR Association, Gothenburg, Sweden

Email: rafiq@lehigh.edu

## Abstract

A goal of this research project is to describe the temporal evolution of the electron temperature profiles in high collisionality NSTX H-mode discharges. Gyrokinetic simulations indicate that microtearing modes (MTMs) are a source of significant electron thermal transport in these discharges. In order to understand the effect MTMs have on transport and, consequently, on the evolution of electron temperature in NSTX discharges, a reduced transport model for MTMs has been developed. The dependence of the MTM real frequency and growthrate on plasma parameters, appropriate for high collisionality NSTX discharges, is obtained employing the new MTM transport model. The dependencies on plasma parameters are compared and found to be consistent with MTM results obtained using the gyrokinetic GYRO code. The MTM real frequency, growthrate, magnetic fluctuations and resulting electron thermal transport are examined for high collisionality NSTX discharges in systematic scans over the relevant plasma parameters. In earlier studies it was found that the version of the Multi-Mode (MM) transport model, that did not include the effect of MTMs, provided a suitable description of the electron temperature profiles in high collisionality standard tokamak discharges. That version of the MM model included contributions to electron thermal transport from the ion temperature gradient, trapped electrons, kinetic ballooning, peeling ballooning, collisionless and collision dominated MHD modes, and electron temperature gradient modes. When the MM model, that includes transport associated with MTMs, is installed in the TRANSP code and is utilized in studying electron thermal transport in high collisionality NSTX discharges, it is found that agreement with the experimental electron temperature profile is significantly improved.

## 1. INTRODUCTION

The ability to understand the physics involved in fusion plasmas, and in particular transport, requires integrated predictive simulations where all the relevant interactive physics is included. The simulations need to be carried out for the duration of the existence of the plasma, that is, for time periods ranging from seconds to thousands of seconds. Thousands of processors, running for many days, are required to carry out a few microsecond simulation of plasma turbulence using gyrokinetic models. Therefore, it is not possible to carry out the required integrated simulations using first principal physics. Consequently, it is of the utmost importance to have fluid or unified fluid/kinetic physics based reduced transport models that can be utilized in integrated physics simulations.

Microtearing modes (MTMs) have been identified as a source of significant electron thermal transport in tokamak discharges [1,2]. In order to understand how MTMs affect transport and consequently the evolution of electron temperature in tokamak discharges, the reduced transport model for microtearing modes has been developed [3] for use in integrated predictive modeling studies. In high collisionality NSTX H-mode discharges the ion thermal transport is generally near neoclassical levels. However, it is found that the electron thermal transport is anomalous and can limit the overall global energy confinement scaling [4]. Gyrokinetic simulations have indicated that MTMs are a source of significant electron thermal transport in these discharges [5]. In the previous publications [2], the ratio of magnetic fluctuations, associated with microtearing modes, to the magnetic field is assumed to be approximately equal to the ratio of electron gyroradius to the electron temperature gradient scale length. This assumption is based on a mixing length estimate, which provides a reasonable estimate for the saturated amplitude for temperature gradients that are sufficiently greater than the linear threshold. However, the mixing length estimate does not capture the dependence of the microtearing mode contribution to electron thermal transport on other parameters such as collisionality, plasma beta, and mode wavenumber. Therefore, transport models that rely on the simplified saturation estimate are incapable of reproducing the correct scaling dependence on these parameters, which illustrates the need for an improved saturation model.

In Sec.2, the MTM reduced transport model, developed in Ref. 3, is summarized. In Sec. 3, the dependence of the MTM real frequency and growthrate on plasma parameters, appropriate for high collisionality NSTX

discharges, is obtained employing the new MTM transport model. The dependencies on plasma parameters are compared with MTM results obtained using the gyrokinetic GYRO code. In Sec. 4, the dependence of the saturated amplitude of the magnetic fluctuation strength on different plasma parameters is shown. The dependence of the microtearing mode real frequency, growthrate, magnetic fluctuation, and electron thermal diffusivity on NSTX prescribed plasma profiles is also shown in Sec. 5. In Sec. 6, predictive simulation of the electron temperature profile of high collisionality NSTX plasmas is presented with and without including a component of MTM reduced transport model in the TRANSP code. The effects of microtearing modes on electron thermal transport in NSTX discharges are summarized in Sec. 7.

## 2. DESCRIPTION OF REDUCED MICROTEARING MODE ANOMALOUS TRANSPORT MODEL

In order to understand how microtearing modes affect transport and, consequently, the evolution of electron temperature in tokamak discharges, a reduced transport model has been developed [3] for use in integrated predictive modeling studies. The electron momentum and density equations, Maxwell's equations, Ampere's law, and quasi-neutrality condition were employed in the development. A unified fluid/kinetic approach was used which included nonlinear effects due to electrostatic and magnetic fluctuations, as well as effects due to collisionality, electron temperature and density gradients, and arbitrary curvature. An iterative approach was applied to calculate the nonlinear distribution function, which, in turn, was used to calculate the nonlinear parallel current in obtaining a nonlinear dispersion relation. The influence of third order nonlinear effects on a multi-wave system was considered, and the third order effects provided a possible mechanism for the temporal saturation of the microtearing instability. The envelope equation for the nonlinear microtearing modes was introduced, which provided the initial linear growth and the final stabilization, and was used to calculate the saturation level of the nonlinear microtearing instability. The electron thermal diffusivity due to microtearing modes was then obtained in terms of the saturated amplitude of the magnetic fluctuation strength.

## 3. COMPARISON OF RESULTS OBTAINED USING MTM REDUCED TRANSPORT MODEL AND THE GYROKINETIC GYRO CODE

A selection of results is presented in this section in which linear microtearing mode eigenvalues are compared with the corresponding values of the gyrokinetic code GYRO. The dependence on the wavenumber,  $k_y \rho_s$ , of the normalized growthrate ( $\gamma a / c_s$ ) of the most unstable microtearing mode and the normalized microtearing mode real frequency ( $\omega_r a / c_s$ ), associated with the most unstable mode, is shown in Fig. 1. These results are found to be consistent with microtearing mode results obtained using the gyrokinetic code GYRO. The plasma parameters values correspond to an NSTX Discharge 120968 are used to obtain the results shown in Fig. 1.  $R = 0.94$  m,  $a = 0.62$  m,  $r_{\min} = 0.37$  m,  $B_T = 0.35$  T,  $\beta_e = 0.09$ ,  $q = 1.7$ ,  $\hat{s} = 1.7$ ,  $T_e = 0.45$  keV,  $k_y / k_x = 0.2$ ,  $n_e = 6.0 \times 10^{19} \text{ m}^{-3}$ ,  $g_{Te} = R / L_{Te} = 4.1$ ,  $g_{ne} = R / L_{ne} = 0$ . This shot is a part of  $\nu_*$  and  $\beta$  dimensionless confinement scaling studies.

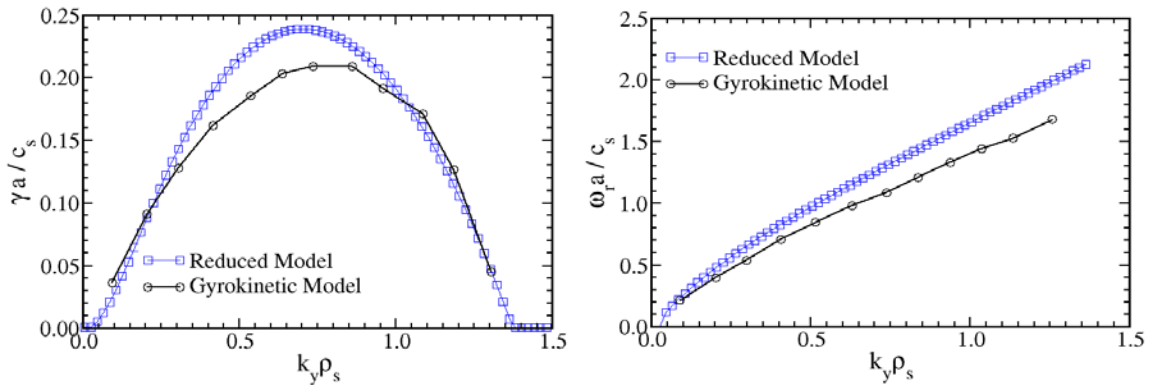


FIG. 1. Normalized microtearing mode real frequency,  $\omega_r a / c_s$  (left panel), and growthrate,  $\gamma a / c_s$  (right panel), are plotted as a function of  $k_y \rho_s$ . Results obtained using the reduced MTM model is indicated by a square-dashed line and the gyrokinetic results are indicated by a circle-dashed line.

It is shown in Fig. 1 (left panel) that the maximum growthrate of the most unstable microtearing mode occurs at  $k_y \rho_s = 0.67$ . The microtearing modes are found to be stabilized for both shorter and longer wavelengths due to the effects of field line bending. In Fig. 1 (right panel), it is shown that the microtearing mode real frequency associated with the most unstable mode increases with an increasing electron temperature gradient. The positive

sign of the real frequency indicates that the microtearing modes propagate in the electron diamagnetic drift direction.

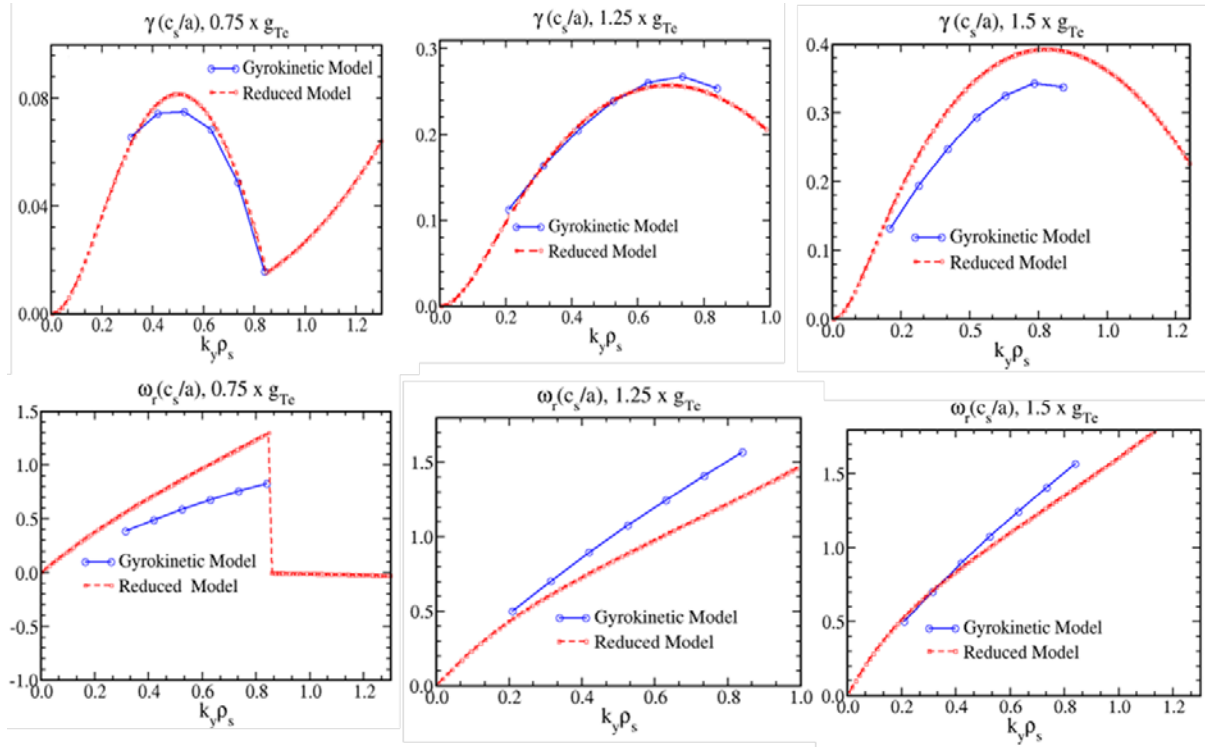


FIG 2: Normalized microtearing mode growthrate and real frequency are plotted as a function of  $k_y \rho_s$  as normalized electron temperature gradient is varied between  $0.7 - 1.5 \times$  the experimental value. Results obtained using the Gyrokinetic model are indicated by a circle-dashed line and the reduced MTM model results are indicated by a square-dashed line.

In Fig. 2, the dependence of the microtearing mode growthrate of the most unstable mode and the associated real frequency is shown as a function of  $k_y \rho_s$  for gyrokinetic and reduced transport models as normalized electron temperature gradient is varied between  $0.7 - 1.5 \times$  the experimental value. It is shown that the maximum growthrate increases as the electron temperature gradient increases, indicating that these modes are driven by the electron temperature gradient. The location and magnitude of the largest growthrate of the most unstable microtearing mode are found to be increasing with increasing the value of the electron temperature gradient, which is successfully captured by the reduced MTM model. The most unstable MTM modes are found  $k_y \rho_s \approx 0.4 - 0.8$ , which indicates that MTM is short wavelength ion scale electromagnetic instability that is driven by the electron temperature gradient.

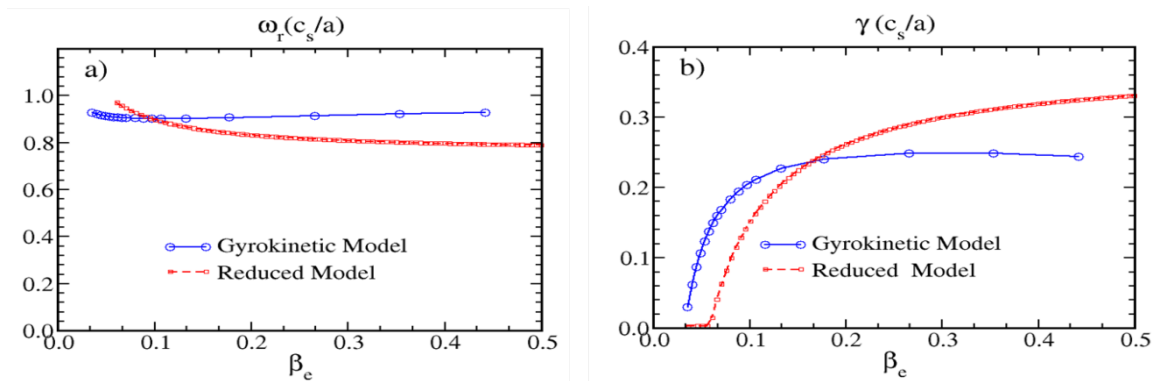


FIG. 3 Normalized microtearing mode real frequency,  $\omega_r a/c_s$ , and growthrate,  $\gamma a/c_s$ , are plotted as a function of  $\beta_e$ . Results obtained using the gyrokinetic model is indicated by a circle-dashed line and the reduced MTM model results are indicated by a square-dashed line.

In Fig. 3, reduced model MTM linear real frequency and growthrate as a function of  $\beta_e$  is compared with gyrokinetic code GYRO linear real frequency and growthrate. For low values of plasma  $\beta_e$ , the growthrate

increases with increasing  $\beta_e$ , but then it saturates for higher values of  $\beta_e$ . The real frequency is found to be almost independent of  $\beta_e$  in both the reduced and gyrokinetic model. The MTM instability threshold in electron beta is found to be around  $\beta_e = 3.0\%$ , while the local experimental value of electron beta is  $9.0\%$ . Moderate destabilization with  $\beta_e$  in experimental range is qualitatively consistent with the weak confinement scaling  $\Omega \tau_E = \beta^{-0.1}$  observed in NSTX experiment.

In Fig. 4, the dependence of the microtearing mode real frequency of the most unstable mode and the associated growthrate are presented as a function of normalized collision frequency and is compared with gyrokinetic code GYRO MTM linear real frequency and growthrate. The real frequency of MTM is found to be increasing with collision frequency. The maximum growthrate is found for moderate values of collision frequency. The nonmonotonic dependence of growthrate on  $v_{ei}$  is consistent with gyrokinetic simulations. However, the cutoff in growthrate for large values of  $v_{ei}$  is found earlier in the reduced model as compared to the gyrokinetic results. The growthrate decreases with decreasing  $v_{ei}$  is consistent with the dependence on collisionality is observed in the NSTX discharges [4].

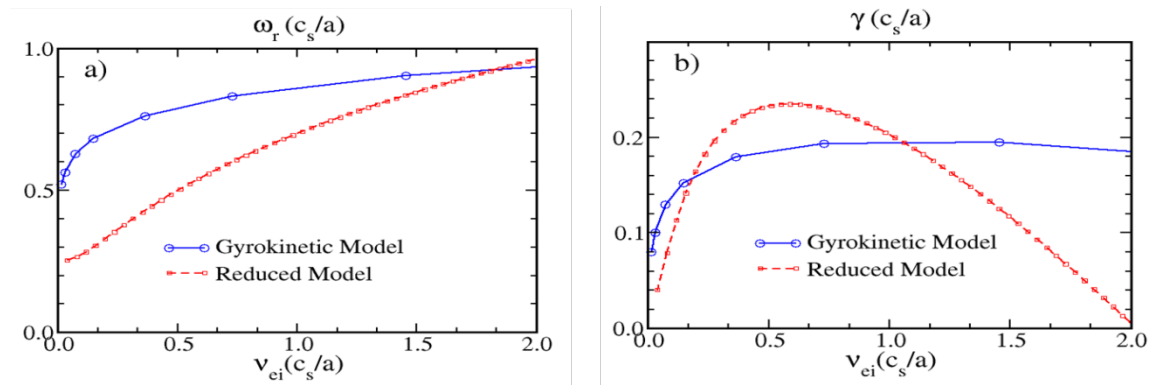


FIG. 4 a) Normalized microtearing mode real frequency,  $\omega_r a/c_s$ , and b) growthrate,  $\gamma a/c_s$ , are plotted as a function of  $v_{ei} a/c_s$ . Results obtained using the reduced MTM model is indicated by a square-dashed line and the gyrokinetic results are indicated by a circle-dashed line.

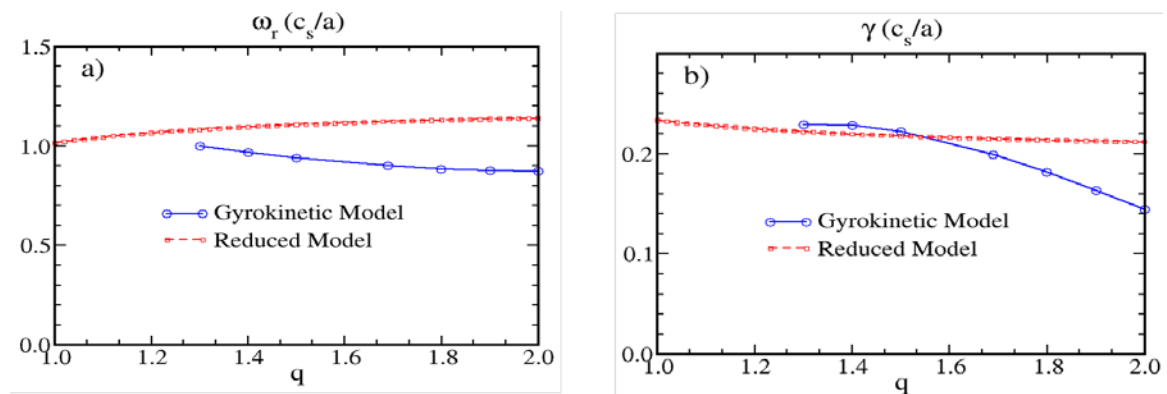


FIG. 5 a) Normalized microtearing mode real frequency,  $\omega_r a/c_s$ , and b) growthrate,  $\gamma a/c_s$ , are plotted as a function of magnetic- $q$ . Results obtained using the reduced MTM model is indicated by a square-dashed line and the gyrokinetic results are indicated by a circle-dashed line.

In Fig. 5, the normalized growthrate of the most unstable microtearing mode and the associated real frequency are shown as a function of the magnetic- $q$ . Although the magnitude of real frequency and growthrate in reduced and gyrokinetic models are not very different, but the significant decreasing of growthrate for larger values of magnetic- $q$  in the gyrokinetic model results is not captured by the reduced model. The safety factor in the reduced microtearing mode derivation enters in the estimation of parallel wavevector,  $k_{\parallel}$  and in the average magnetic curvature formula. The simple estimation of parallel wavevector [4], which does not depend on toroidal geometry, might be a reason of not capturing the significant decreasing trend of growthrate for large values of magnetic- $q$ .

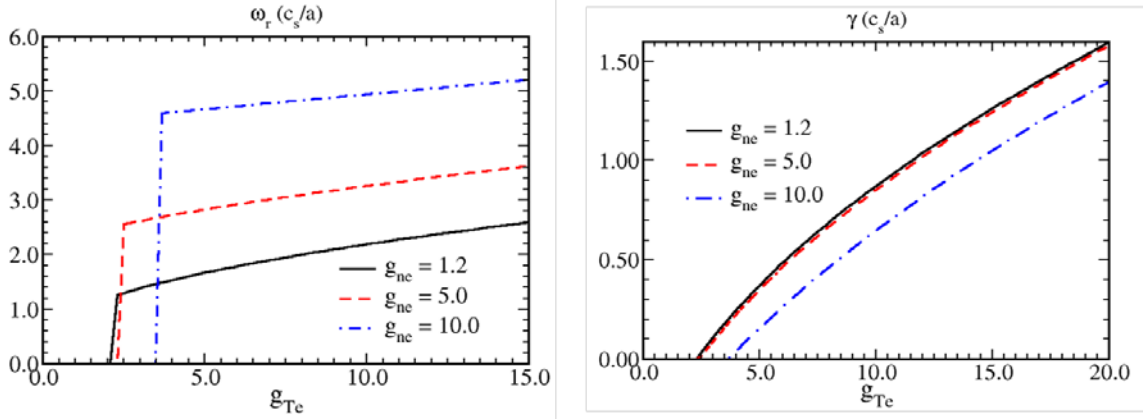


FIG. 6 (a) The dependence of the normalized real frequency,  $\omega_r a/c_s$ , of the most unstable microtearing mode and (b) the associated normalized growthrate,  $\gamma a/c_s$ , are shown as a function of the normalized temperature gradient,  $g_{Te}$ . The solid curves are for the normalized density gradient,  $g_{ne} = 1.2$ ; dashed curves are for  $g_{ne} = 5.0$ ; and the dotted-dashed curves are for  $g_{ne} = 10.0$ .

The real frequency of the most unstable microtearing mode and growthrate associated with that mode is plotted using the reduced MTM model in Fig. 6 as a function of normalized temperature gradient  $g_{Te}$  for three values of normalized electron density gradient. It is found that the microtearing mode growthrate and corresponding real frequency both increase as the electron temperature gradient increases. It is also found that nonzero temperature gradient is required for the microtearing mode instability. The threshold in electron temperature gradient increases as electron density increases, while growthrate is found to be decreasing with increasing density gradient. The NSTX experimental value of electron temperature gradient of microtearing mode is larger than the inferred linear threshold found in the Fig. 6.

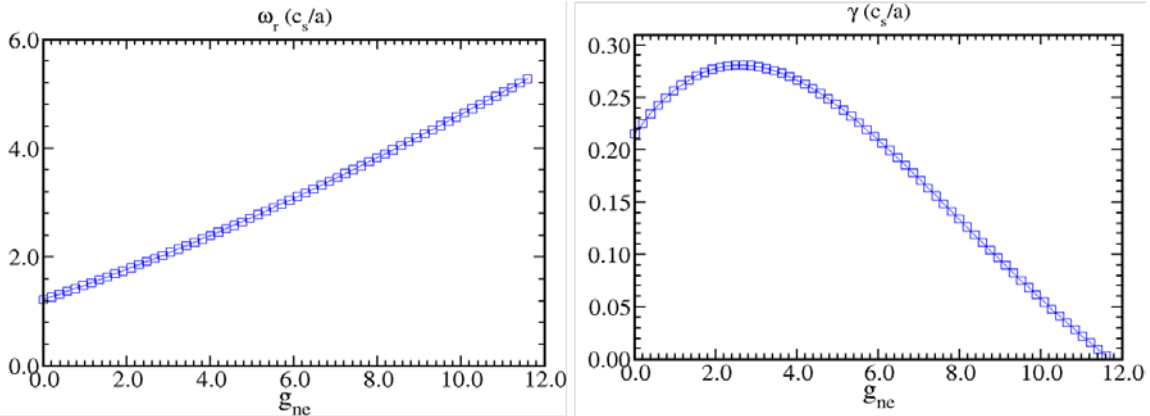


FIG. 7 The dependence of the normalized real frequency,  $\omega_r a/c_s$ , of the most unstable microtearing mode and the associated normalized growthrate,  $\gamma a/c_s$ , are shown as a function of the normalized temperature gradient,  $g_{ne}$ .

The normalized real frequency of the most unstable microtearing mode and the associated growthrate is shown as a function of normalized density gradient,  $g_{ne}$ , in Fig. 7. The real frequency is found to be increasing with increasing density gradient. The maximum growthrate is found for moderate values of the density gradient. The both small and large density gradient is found to be stabilizing. The large density gradient  $g_{ne} = 12.0$ , stabilizes microtearing mode completely. The density profile in the core of NSTX discharges is flat, so less stabilization is expected in the experiments from density gradient.

The normalized growthrate versus  $Z_{eff} v_{ei}/\omega_r$  is plotted in Fig. 8. It is found that as collision frequency decreases the MTM growthrate decreases as well. This scaling trend is qualitatively consistent with the global energy confinement trend,  $\Omega \tau_E = \nu_*^{-0.95}$  observed in NSTX analysis. This behavior is opposite to the drift wave instabilities where collisionality tends to provide a stabilizing influence to trapped electron mode, which otherwise enhance the ion and electron temperature gradient instability in the collisionless limit. The peak MTM growthrate occurs around  $Z_{eff} v_{ei}/\omega_r \approx 2$ . A slight shift in the peak value towards large collisionality is found when magnetic curvature,  $\omega_{De}$ , is ignored.

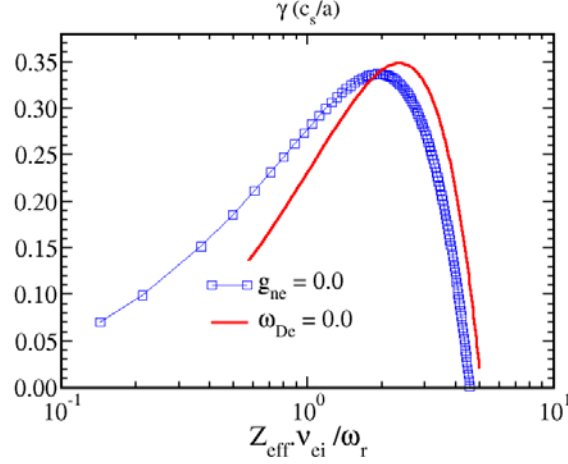


FIG. 8 Normalized microtearing mode growth rate,  $\gamma a/c_s$  versus  $Z_{\text{eff}} v_{ei}/\omega_r$ . The square dashed curve is for  $g_{ne} = 0$  and  $\omega_{De} \neq 0$ ; the solid curve is for  $g_{ne} = 0$  and  $\omega_{De} = 0$ .

#### 4. MAGNETIC FLUCTUATION DEPENDENCE ON $\beta_e$ , TEMPERATURE AND DENSITY GRADIENTS

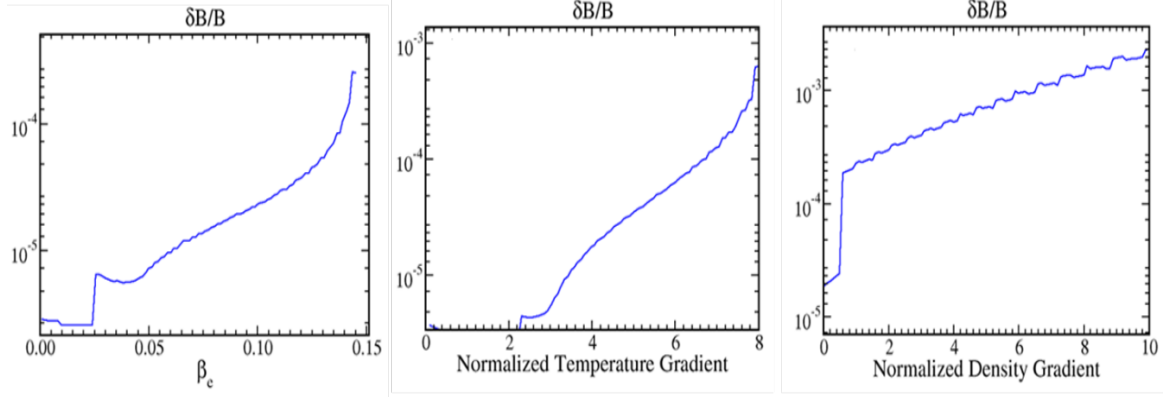


FIG.9 Normalized magnetic fluctuation,  $\delta B/B$ , is plotted as a function of  $\beta_e$ , normalized temperature gradient,  $g_{Te}$ , and normalized density gradient,  $g_{ne}$ .

The dependence of the magnetic fluctuation strength,  $\delta B/B$ , due to microtearing mode as a function of  $\beta_e$ , normalized temperature gradient,  $g_{Te}$ , and normalized density gradient,  $g_{ne}$  is plotted in Fig. 9. The magnetic fluctuation clearly shows dependence on  $\beta_e$ , temperature and density gradients. The magnetic fluctuation is found to increase with increase in  $\beta_e$ , temperature and density gradient. In the previous MTM publications [2] the unstable microtearing mode is assumed to saturate  $\frac{\delta B}{B} \approx \rho_e/L_{Te}$  and is incapable of capturing magnetic fluctuation dependencies shown in Fig. 9. Note, in contrast, the computation of magnetic fluctuations here makes use of the nonlinear microtearing mode envelope equation [Eq. (55) of Ref. 3].

#### 5. BEHAVIOR OF MTM MODEL FOR NSTX PRESCRIBED PROFILES

In Fig. 10, the magnetic-q, electron temperature, electron density, the normalized temperature and density gradient profiles are plotted for an NSTX tokamak discharge. The growth rates, real frequency, and values of  $k_y \rho_s$  associated with the most unstable mode are plotted in Fig. 11 (a-c). The magnetic fluctuation strength,  $\delta B/B$  and microtearing electron thermal diffusivity,  $\chi_e (m^2/s)$  profiles are plotted in Fig. 11(d-e).

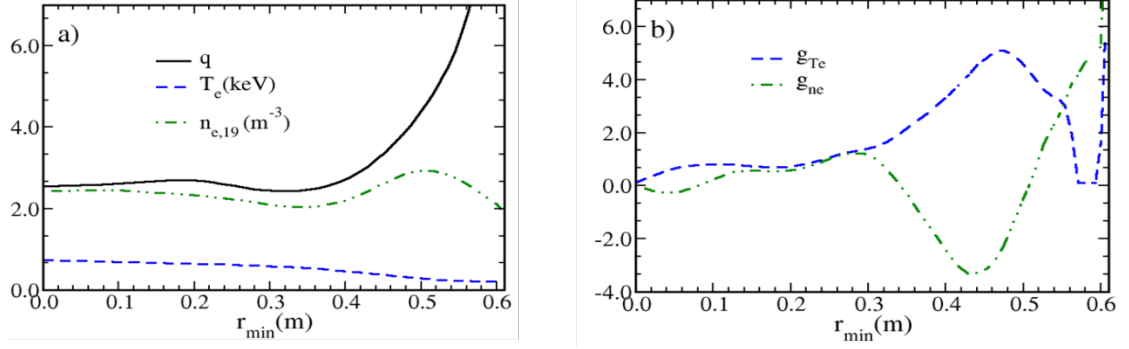


FIG. 10 (a) Equilibrium NSTX H-mode tokamak profiles, magnetic- $q$ , electron temperature ( $T_e$ ) and electron density ( $n_{e,19}$ ); (b) normalized temperature and density gradient is plotted as a function of radius.

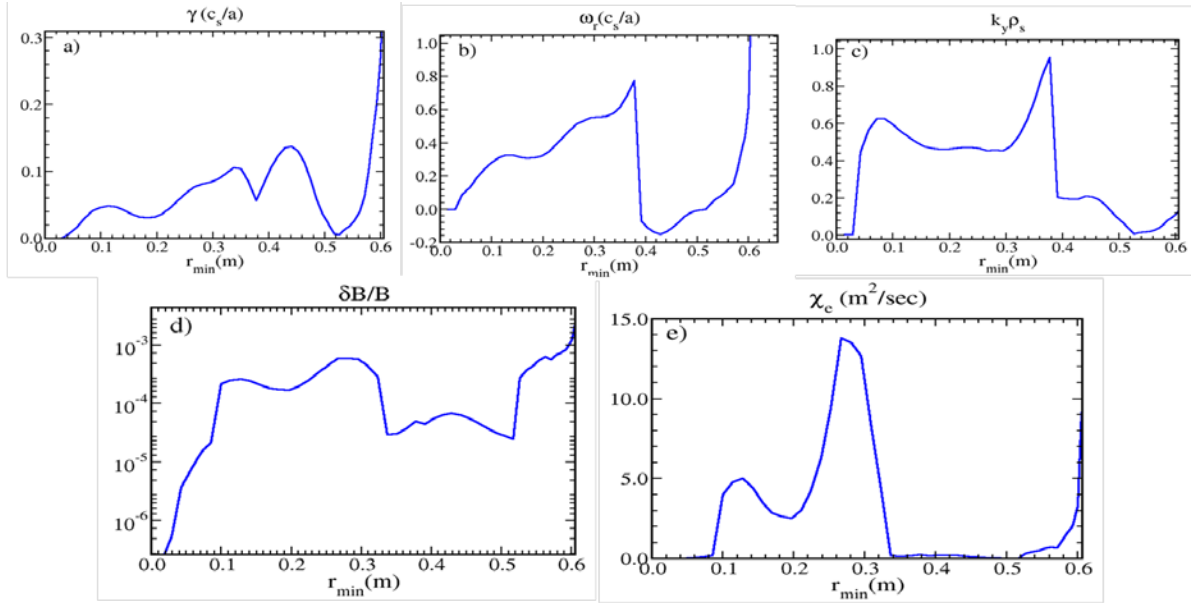


FIG. 11 (a) Normalized microtearing mode growthrate,  $\gamma a/c_s$ . (b) Normalized real frequency,  $\omega a/c_s$ . (c) The corresponding values of  $k_y \rho_s$ . (d) Normalized magnetic fluctuation strength,  $\delta B/B$ . (e) Electron thermal diffusivity,  $\chi_e$  is plotted as a function of radius.

The microtearing mode is found to be unstable linearly at most of the radius. However, the growthrate is found to be larger in the region of a large temperature gradient and found to be small in the region of a small temperature gradient. A change in the direction of the mode frequency is found from electron diamagnetic direction to the ion diamagnetic direction with the change in the sign of the normalized density gradient. The values of  $k_y \rho_s < 1.0$ , associated with the most unstable microtearing mode at each radius, indicate that these unstable modes are ion scale modes over the whole plasma radius including the plasma core region. The saturated amplitude of the magnetic fluctuation strength, which depends upon the growthrate and real frequency of the most unstable mode and as well as on their sidebands in the  $k_y \rho_s$  spectrum is found  $\frac{\delta B}{B} \approx 10^{-4} - 10^{-3}$ , which is consistent with the gyrokinetic estimation of magnetic fluctuation. The electron thermal diffusivity that occurs due to the magnetic fluctuations is found to be large in the region of moderate collisionality as is shown in Fig. 11e. The magnetic fluctuations and the thermal diffusivity are also found to be large at the edge region of the plasma due to a large value of temperature and density gradients.

## 6. PREDICTED AND MEASURED ELECTRON TEMPERATURE FOR A HIGH $\nu^*$ NSTX DISCHARGE

A goal of this research project is to describe the evolution of the electron temperature profiles in high collisionality NSTX discharges. In earlier studies it was found that the version of the Multi-Mode (MM) transport model, that did not include the effect of microtearing modes, provided a suitable description of the electron temperature profiles in high collisionality standard tokamak discharges [6,7]. That version of the MM

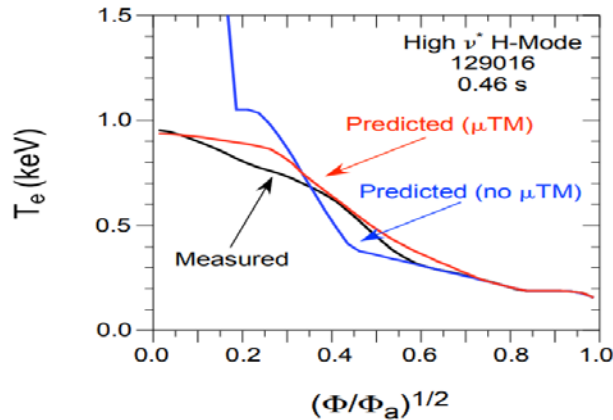


FIG.12. The simulated and experimental electron temperatures for the high  $\nu^*$  NSTX discharge, 120916, with and without the contribution of transport associated with microtearing modes, as a function of the normalized square root of toroidal

model included contributions to electron thermal transport from the ion temperature gradient, trapped electrons, kinetic ballooning, peeling ballooning, collisionless and collision dominated MHD modes, and electron temperature gradient modes [8]. When the MM model, that includes transport associated with microtearing modes, is installed in the TRANSP code and is utilized in studying electron thermal transport in NSTX discharges, it is found, as shown in Fig. 12, that agreement with the experimental electron temperature profile is significantly improved in a high collisionality discharge. Future research will involve improving the electron thermal transport model for low collisionality NSTX discharges.

## 7. SUMMARY

Reduced microtearing mode model, which has been developed for use in integrated predictive modeling studies, employed a unified fluid/kinetic approach to derive the nonlinear dispersion relation. This approach augmented the kinetic description and allowed the inclusion of nonlinear effects due to magnetic fluctuations. The objective is to improve the prediction of the evolution of the plasma in devices in which microtearing modes have a significant role. The linear dependence of the real frequency and growthrate of microtearing modes on plasma parameters, appropriate for high collisionality NSTX discharges, is investigated. The dependence of the real frequency and growthrate on plasma parameters obtained using the reduced transport model for microtearing modes is compared and found to be consistent with the microtearing mode results obtained using the gyrokinetic code GYRO. It is found that the temperature gradient along with the collision frequency and plasma beta are sufficient for MTM to become unstable in an NSTX high collisionality discharge. The MTM saturated magnetic fluctuation strength and the corresponding electron thermal diffusivity are calculated. The diffusivity is found to be large in the regions of either moderate collisionality or large gradients. When the MM model, that includes transport associated with microtearing modes, is installed in the TRANSP code and is utilized in studying electron thermal transport in NSTX discharges, it is found that agreement with the experimental electron temperature profile is significantly improved in a high collisionality discharge.

## ACKNOWLEDGEMENTS

This work is supported by the U.S. Department of Energy, Office of Science, under Award Number DE-SC0013977, DE-FG02-92ER54141, and DE-AC02-09CH11466.

## 8. REFERENCES

- [1] Hazeltine, R. D., Dobrott, D., and Wang, T. S. Phys. Fluids 18 (1975) 1778.
- [2] Drake, J. F., Gladd, N. T., Liu, C. S., and Chang, C. L., Phys. Rev. Lett. 44 (1980) 994.
- [3] Rafiq, T., Weiland, J., Kritz, A.H., Luo, L., and Pankin, A. Y., Phys. Plasmas 23 (2016) 062507.
- [4] Kaye, S.M., Levinton, F.M., Stutman, D., Tritz, K., Yuh, H., *et al.*, Nucl. Fusion 47 (2007) 499.
- [5] Guttenfelder, W., Candy, J., Kaye, S. M., Nevins, W. M., Bell, *et al.*, Phys. Plasmas 19 (2012) 022506.
- [6] Bateman, G., Bandrés, M. A., Onjun, T., Kritz, A. H., and Pankin, A., Phys. Plasmas 10 (2003) 4358.
- [7] Rafiq, T., Kritz, A. H., Tangri, V., Pankin, A. Y., Voitsekhoitch, I., Budny, R.V., Phys. Plasmas 21 (2014) 122505.
- [8] Rafiq, T., Weiland, J., Kritz, A. H., Luo, L., Pankin, Phys. Plasmas 20 (2013) 032506.